Patient Adapted SAR Calculation on a Parallel Transmission System

I. Graesslin[1], H. Homann[2], S. Biederer[3], P. Börnert[1], G. Mens[4], and P. Harvey[4]
[1]Philips Research Laboratories, Hamburg, Germany, [2]Institute of Biomedical Engineering, Karlsruhe Institute of Technology, Germany, [3]Institute of Medical Engineering, University of Lübeck, Lübeck, Germany, [4]Philips Healthcare, Best, Netherlands

Introduction For in vivo parallel transmit MRI experiments, conformity of the RF waveforms with existing SAR limits [1] has to be verified to assure patient safety. The parallel transmit system presented in this paper is capable of carrying out patient-adapted SAR calculations in real-time before scanning. This safety concept comprises two scan modes. In the first mode, a worst-case SAR model is used, representing various patient anatomies and body positions in the MR scanner. In this mode, survey scans can be performed to collect patient-specific information. In the second mode, a selected body model of anatomy and body pose comparable to the patient is used for SAR calculation. This allows for a more accurate SAR estimation and hence provides more design freedom in SAR-limited MR sequences.

Methods The safety concept was implemented on an eight-channel transmit 3T MRI system [2] (based on Achieva, Philips Healthcare, Netherlands). First, survey scans can be acquired using the worst-case SAR mode. In this study, chemical-shift encoded scans were acquired for estimation of the body's water-fat-ratio. For the selection of a patient-adapted SAR model, further relevant patient-specific information was obtained from the scanner's host system (cf. Fig.1), including the patients sex, body height and weight as well as the body orientation and the anatomical region of the scan. Based on these parameters, a suitable patient-specific SAR model was selected from a database of pre-simulated body models [3]. This selection was made from the subset of models that had identical "hard parameters" (i.e. sex and body position) and using the similarity measure $d_{p,m} = \Sigma a_i | p_{i,m} - p_{i,p} |/p_{i,m}$ for comparing the "soft parameters" (i.e. weight, height, and water-fat-ratio), where the p_i are the *i*-th parameter of the model and the patient and the a_i are some weighting factors.

The database was generated for different body models by the following processing steps according to [3]: Whole-body 3D MR scans were acquired from multiple volunteers (age 29-43years, weight 65-86kg) with an isotropic resolution of 5mm. Three-echo DIXON sampling was applied for subsequent water/fat segmentation. Written informed consent was obtained from all volunteers scanned for this body model library. The data was segmented into 3 tissue types, namely water, fat, and lung tissue. In the next step, the E-fields were determined by FDTD simulation ("XFDTD MicroCluster", Remcom Inc., USA) for all dielectric body models including the "Visible Human Male" [4] for comparison. The body models were placed in a model of an ideally decoupled 3T eight-channel body coil [5] at 18 different patient positions in the coil. The E-fields were then pre-calculated for all bio-mesh models and for each coil element of the TX array. The E-fields were then averaged according to [6] and finally stored in the database, the so-called Q-matrix data base (QM in Fig.1). For the SAR calculation, the fields were superimposed weighted with the RF pulse.

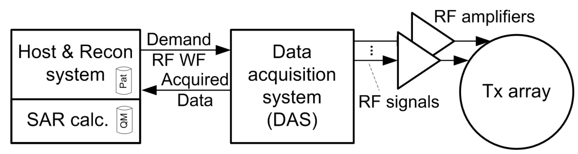

Fig. 1: SAR calculation is carried on the host, which uses pre-calculated bio-mesh models from a database. The model selection is based on patient specific information. The host sends the demand RF waveforms (WFs) to the data acquisition system (DAS).

The visible human model comprises roughly 750k cells and the patient-specific models comprise 310k-540k cells. For increased efficiency, a so called clustering process as proposed by [7] was used. This reduces the models to about 80-5,000 cells when allowing for an SAR overestimation of 10%. This procedure was carried out for each of the 18 bed positions. In a second step the clustering was applied on all z-positions as well as over all models to generate the worst-case model. Depending on the amount of SAR calculations to be carried out, the processing is carried out in SW on a CPU or on a high performance graphics card (GeForce GTX280, EVGA® Corporation, USA) with 240 processors resulting in a sub-millisecond processing time. The graphics card was integrated into the system. The Q-matrices are cached on the graphics card to minimize the computational latency. The model selection and SAR calculation mechanisms are fully integrated into the scanner GUI and can be applied for all protocols available on the scanner including multi-channel spatially selective RF pulses.

Results and Discussion For selection of an appropriate body model, the water-fat-ratios from a survey scan were used in addition to the parameters obtained from the scanner's host system. The water-fat-ratios, calculated from the whole body and from a single slice only, are shown in Tab. 1 exemplarily for some of the volunteers. The correlation coefficient between the values was 0.89. This indicates that a characterization of the patient's body fat content from a 2D water-fat-separated survey image might be a good estimation for future automation of the calculation of the water-fat-ratio. A good agreement exists between the single slice and whole body water-fat-ratios for the volunteer models. Fig. 2 shows the maximum local SAR for an RF shimming application as a function of the admissible normalized root mean square error (NRMSE) of the effective TX field. In this example, the limiting SAR values occurred in the extremities, while the local torso SAR may be the limiting factor in other cases. The local extremities SAR values obtained from the Visible Human model exceed these values by a factor of approximately two. This may be explained by the unfavorable body position of the Visible Human model with its hands placed on the body such that a current loop is formed as well as the close proximity to the TX elements. Fig. 3 shows the dependence of the maximum local SAR values on the position of the model relative to the body coil. The extremity SAR shows strong deviations depending on the position. This margin may be exploited in the scan design when using patient-adapted models instead of the worst-case approach. As most scans at 3T are SAR-limited, a correct SAR calculation or a close approximation is important and preferably the actual patient position should be taken into account.

Conclusion Successful integration of a worst-case as well as patient-adapted SAR calculation in sub-milliseconds was demonstrated for a parallel transmit platform. Selection of patient adapted models based on a similarity measure was introduced. However, the relevant parameters and weighting factors need further investigation. The patient-adapted model allows for an increase of the RF duty cycle due to a better SAR prediction accuracy opposed to using a single generic body model.

Patient-specific selection of an appropriately SAR model may be of particular interest for situations like imaging of pregnant women or fetal imaging as well as in advanced research. In clinical practice, this may be advantageous: a) for standard systems to enhance the scan time or contrast (e.g. by reduced TR or large flip-angles) and b) for parallel transmit systems to realize advanced SAR management (e.g. targeted hotspot suppression or higher quality RF pulses with higher SAR). For future applications, a survey scan using the worst-case SAR model might even be used to generate individualized anatomical patient models [8].

	Whole body (water/fat)	Abdominal slice (water/fat)
Volunteer 1	78%	73%
Volunteer 2	60%	68%
Volunteer 3	53%	45%
Volunteer 4	50%	46%
Volunteer 5	72%	78%
Volunteer 6	58%	50%

Tab. 1: Water-fat-ratios for different volunteers a) calculated over the whole body, b) calculated from a single abdominal slice.

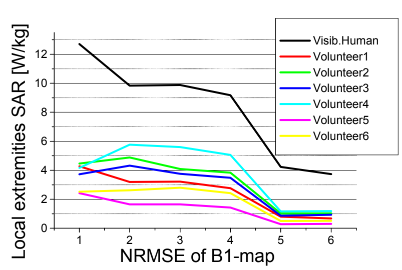

Fig. 2: Comparison of local extremities SAR for the volunteer models and the Visible Human model.

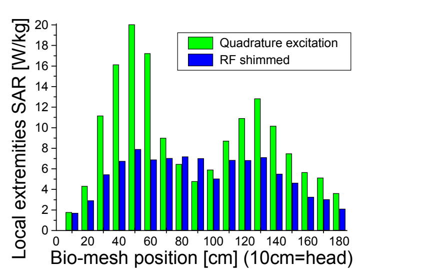

Fig. 3: Position-dependence of the SAR values for the 8-channel body coil for quadrature excitation (emulating a standard body coil) and for RF shimming.

References
[1] IEC [2002] 60601-2-33, 2nd Ed.
[2] Graesslin I, et al. [2006] ISMRM 14:129
[3] Homann H, et al. [2010] ISMRM 18:3874
[4] NLM [1996] "Visible Human Project"
[5] Vernickel P, et al. [2007] MRM 58(2):381-9
[6] IEEE Inc. [2002] Std C95, 3rd Ed.
[7] Gebhardt M, et al. [2010] ISMRM 18:1441
[8] Graesslin I, et al. [2010] ISMRM 18:3873